NMR evidence of a sharp change in a measure of local order in deeply supercooled confined water

F. Mallamace*†‡, C. Corsaro*, M. Broccio*, C. Branca*, N. González-Segredo*§, J. Spooren*, S.-H. Chen†, and H. E. Stanley‡¶

*Dipartimento di Fisica e Consorzio Nazionale Interuniversitario per le Scienze Fisiche della Materia, Universitá di Messina, Villaggio Sant'Agata CP 55, 98166 Messina, Italy; †Department of Nuclear Science and Engineering, Massachusetts Institute of Technology, Cambridge, MA 02139; and ¶Centre for Polymer Studies and Department of Physics, Boston University, Boston, MA 02215

Contributed by H. E. Stanley, May 30, 2008 (sent for review January 8, 2008)

Using NMR, we measure the proton chemical shift δ, of supercooled nanoconfined water in the temperature range 195 K < T < 350 K. Because δ is directly connected to the magnetic shielding tensor, we discuss the data in terms of the local hydrogen bond geometry and order. We argue that the derivative $-(\partial \ln \delta/\partial T)_P$ should behave roughly as the constant pressure specific heat $C_P(T)$, and we confirm this argument by detailed comparisons with literature values of $C_P(T)$ in the range 290–370 K. We find that $-(\partial \ln \delta/\partial T)_P$ displays a pronounced maximum upon crossing the locus of maximum correlation length at ≈240 K, consistent with the liquid-liquid critical point hypothesis for water, which predicts that $C_P(T)$ displays a maximum on crossing the Widom line.

configurational specific heat | nuclear magnetic resonance | proteins | proton chemical shift

Unlike most fluids, water displays anomalies in thermodynamical properties such as compressibility, isobaric heat capacity, and thermal expansion coefficient, and their explanation on molecular basis remains a challenge (1–3). One hypothesis that has received support from various theoretical studies (4–7) is the liquid-liquid (LL) critical point hypothesis, but a proper test can be obtained only by studying the properties of liquid water well below its homogeneous nucleation temperature, $T_H = 231$ K. This is made possible by confining water inside nanoporous structures so small that the liquid cannot freeze.

Among recent findings concerning water's dynamical properties at these low temperatures are (8–13): a fragile-to-strong crossover and the violation of the Stokes-Einstein relation, related to the crossing of the Widom line and to the existence of a low-density-liquid-like (LDL-like) local structure. The Widom line is the locus of maximum correlation length in the one-phase region beyond the liquid-liquid critical point, where thermodynamic response functions take their maximum values (12, 13). Scattering experiments (using neutrons and x-rays) have given precise values of the pair correlation function (PCF), providing important benchmarks for testing models of its structure. The PCF represents only an isotropically averaged measure of structure. Thus, in many cases, PCFs may not faithfully reproduce the subtle hydrogen bond geometry responsible for water's thermal anomalies. Our goal in this study is to provide additional information on the local hydrogen bond geometry and, in particular, the average number of the possible configurations of the local molecular hydrogen bonding geometry, by measuring the NMR proton chemical shift δ. If a water molecule in a dilute gas is taken to be an isolated-state reference, the chemical shift δ accounts for the change of the value of the magnetic shielding with respect to that of such a reference. Hence the chemical shift is related to the "non-dilute" or "virial" interaction of a water molecule with its surroundings, providing a picture of the intermolecular geometry (14–19). Originally, it has been proposed, especially in the high temperature regime, that δ represents the number of hydrogen bonds (HB), N_{HB}, with which a water molecule is involved at a certain temperature (20–22). Nowadays it is accepted that, especially after a lot of theoretical and experimental studies, the proton chemical shift of water is a function not only of the number of HB but also of the intermolecular distances and angles: i.e., $\langle N_{HB} \rangle$ (16). Thus, a careful study of δ vs. T gives details of the thermal evolution of the water configurations especially in the supercooled regime where there is the onset of complex clustering phenomena [percolation-like (23, 24)] just driven by the HB interaction (25–30).

We propose here an approach for which the T derivative of the chemical shift can give an estimate of the configurational specific heat and measure the water proton chemical shift as a function of temperature by studying confined water in two different systems recently used to measure water thermodynamical parameters under deep supercooling conditions: (*i*) a micelle-templated mesoporous silica matrix, comprised of quasi-1D cylindrical tubes (MCM-41-S) (8–13, 31), and (*ii*) the hydration water in the protein lysozyme in the temperature range 180 K < T < 360 K, a system also the object of detailed studies by using both theoretical and experimental approaches (32–37).

Fig. 1*A* shows our $\delta(T)$ data in MCM samples, after correcting for the magnetic susceptibility $\chi(T) = \chi_0\rho(T)$. Fig. 1*A* also shows, from the work of Hindman (21), all of the experimentally available $\delta(T)$ data in the temperature range of stable bulk liquid water, and the δ values from $T = 350$ K down to 235 K, of three different samples: large (80–120 μm) and small (10–20 μm) capillaries, and water confined in an emulsion (38). Although for the δ data of refs. 21 and 38, the reference material was CH_4, all measured values, after the proper correction, nicely fall onto a single master curve, whereby the reference system is a water molecule in a diluted gas in supercritical conditions (14). Fig. 1*A* reports such a situation in the range 180 K < T < 370 K and shows agreement between our data and the previous $\delta(T)$ measurements. We see that the behavior of these literature data (circles) is characterized by a continuous increase on decreasing T that becomes more pronounced in the lower temperature region. At lower T the situation changes: on decreasing T there is a round-off in $\delta(T)$ with a possible maximum at ≈215 K. Because different experiments quote (with respect to the isolated water molecule) δ = 7.4 ppm for a single crystal of hexagonal ice I_h (39), our data show that $\delta(T)$ does not evolve in a simple monotonic way from the liquid to the ice phase. The continuous increase in the proton chemical shift with T decreasing down to the supercooled regime, has been originally interpreted in terms of a cooperative increase in HB formation rate.

Author contributions: F.M., S.-H.C., and H.E.S. designed research; F.M., C.C., M.B., C.B., and J.S. performed research; F.M., C.C., M.B., C.B., N.G.-S., and J.S. analyzed data; and F.M., C.C., N.G.-S., and S.-H.C. wrote the paper.

The authors declare no conflict of interest.

Freely available online through the PNAS open access option.

‡To whom correspondence may be addressed. E-mail: francesco.mallamace@unime.it or hes@bu.edu.

§Present address: ETH Swiss Federal Institute of Technology Zurich, Computational Biophysics Lab, Universitaetstrasse 6, CAB E11, 8092 Zurich, Switzerland.

© 2008 by The National Academy of Sciences of the USA

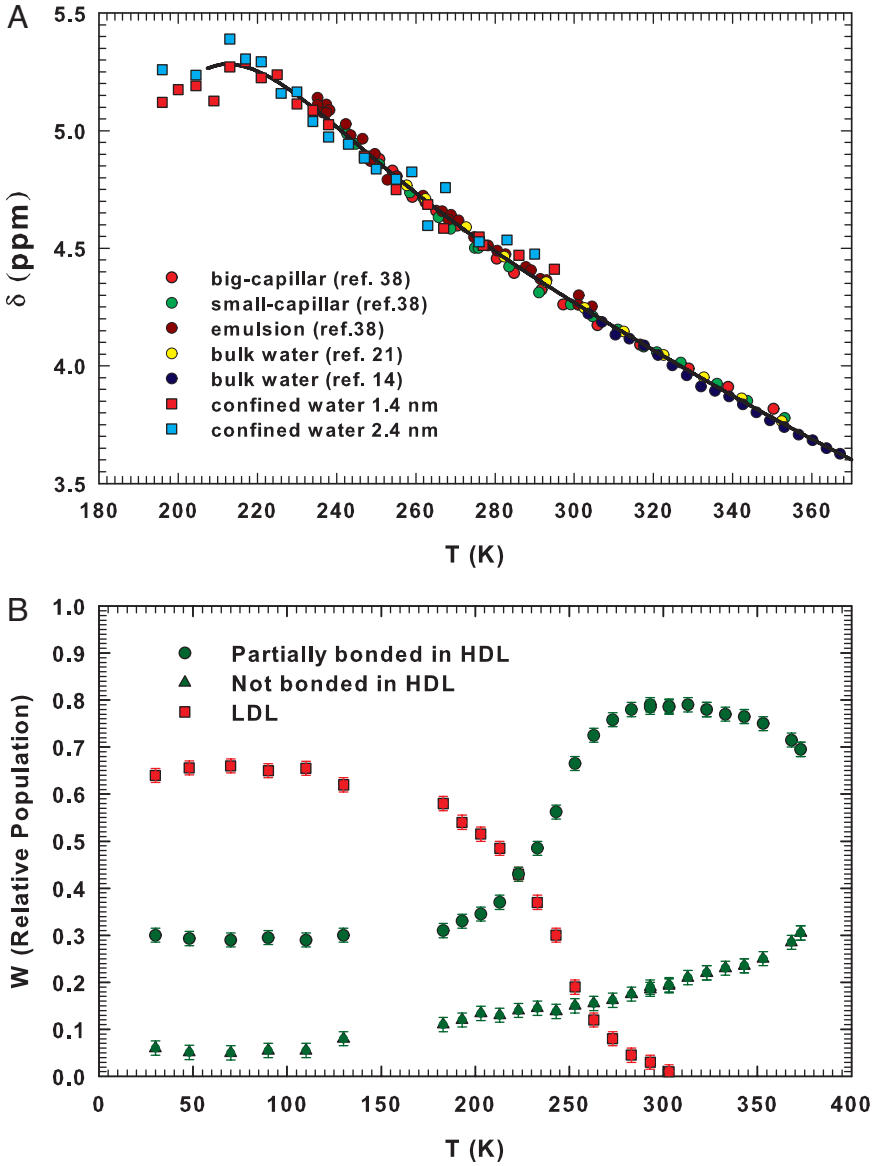

Fig. 1. The proton chemical shift and the relative populations of water. (*A*) Proton chemical shift of water, δ, as a function of temperature. Literature data are plotted as circles, and the present data are plotted as squares symbols. The line is a guide for the eye. (*B*) The relative population of the high density liquid (HDL) and the low density liquid (LDL) water contributions obtained from the Raman and FTIR spectral analysis versus temperature. The HDL and the LDL data are plotted as green and red symbols, respectively. For HDL, the contributions of partially bonded $1 < N_{HB} < 3$ (circles) and not bonded $N_{HB} = 0$ (triangles) water molecules are reported separately. As can be observed, these latter two contributions have opposite behaviors on increasing $T > 300$ K.

Thus, there is a continuous development of a considerable degree of short-range order or "clustering." In addition, because the T region <225 K is dominated by the LDL local structure (11), this confirms the idea that this liquid-water phase has a local geometry different from the high-density liquid (HDL) local structure prevalent in the stable liquid regime.

The recently measured relative population of the two main local structures, LDL-like and HDL-like (11, 40), in the region $30\ \text{K} < T < 373\ \text{K}$, provides a qualitative explanation for the observed $\delta(T)$ (Fig. 1*A*). From a structural point of view, the temperature range can be divided into three intervals:

- $\Re_{\text{HDL}}$ ($T > 250$ K) dominated by molecules with local HDL geometry.
- $\Re_{\text{LDL}}$ ($T \lesssim 220$ K) dominated by local LDL geometry and an intermediate region in which the population of these local geometries are comparable:
- $\Re_{\text{int}}$ ($220\ \text{K} \lesssim T < 250\ \text{K}$).

Visual inspection of $\delta(T)$ shows three different behaviors as temperature decreases in the three different regions: (*i*) a continuous increase in $\Re_{\text{HDL}}$, (*ii*) an inflection point at ≈250 K with a sudden change in the derivative in the $\Re_{\text{int}}$ interval, and finally (*iii*) a flattening at ≈220 K followed by a slow decrease in the $\Re_{\text{LDL}}$ region. These results support a picture in which the main role is played by the LDL and HDL local geometric structure, characterized by different local electronic distributions, thus by different local environments of the hydrogen atom. A proper analysis of their fractional weights allows us to calculate the absolute value of water density $\rho(T)$ in the range $30\ \text{K} < T < 373\ \text{K}$. In addition to the well known maximum at 277 K, there appears a minimum in $\rho(T)$ at 203 ± 5 K (40). Moreover, the coefficient of thermal expansion $\alpha_\rho = -(\partial\rho/\partial T)_P$, related to the cross-correlation between the entropy and volume fluctuations,

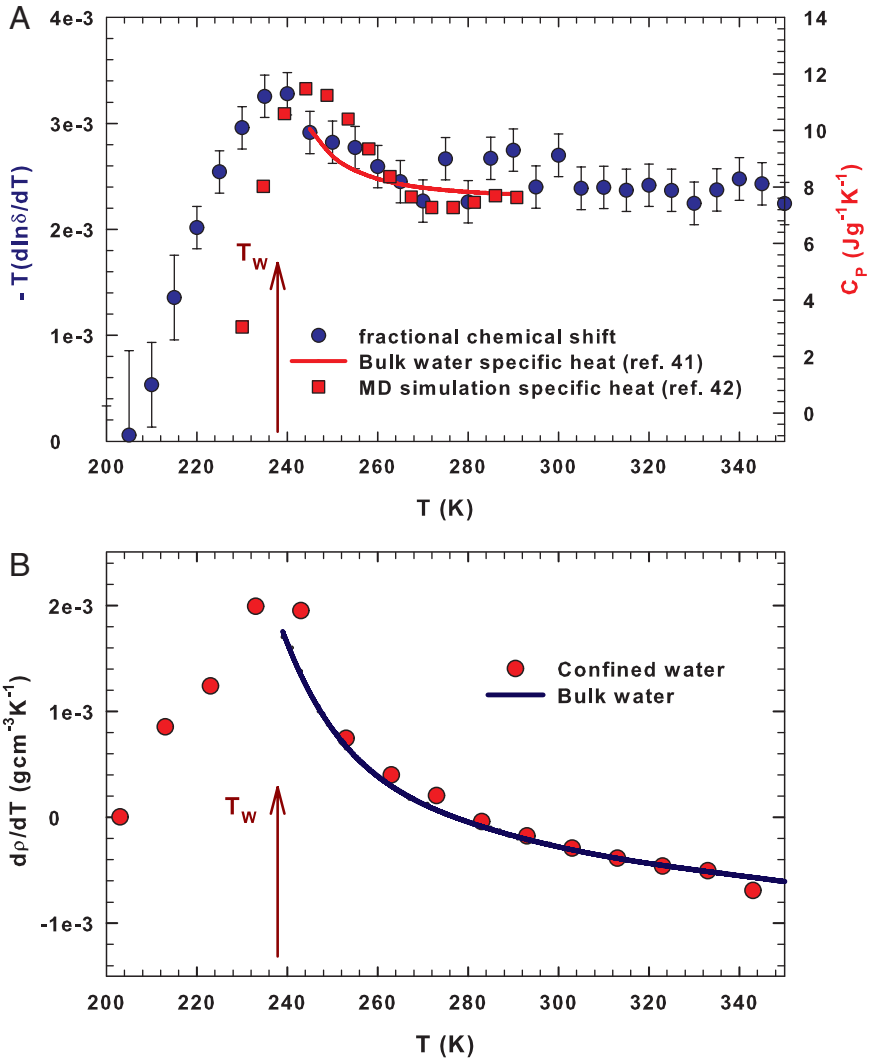

Fig. 2. Measured thermodynamical response functions of water. (*A*) The temperature derivative of the measured fractional chemical shift $-T\partial \ln \delta(T)/\partial T$ (blue symbols, *Left*), the specific heat at constant pressure, C_P (*Right*), measured in bulk water in the supercooled regime (red line, ref. 41), and C_P calculated for the TIP5P model of water (red squares, ref. 42). (*B*) The temperature derivative of the water density (40). The arrows indicate the Widom line temperature T_W.

shows a well defined maximum on crossing the Widom line $T_W(P)$. In the first interval $\mathcal{R}_{HDL}$, in which the normal liquid region (273–353 K) and a region of moderate supercooling lie, $\delta(T)$ increases as T decreases. Both the normal liquid and the supercritical regions have been considered from both the theoretical and experimental points of view to explain as the proton chemical shift reflects the properties of the local order (14, 16, 17) in regions in which there is a direct relation between $\delta(T)$ and the average number of hydrogen bonds $\langle N_{HB}\rangle$, in which a water molecule is involved: $\delta(T) \propto \langle N_{HB}\rangle$. On the basis of the thermal evolution of the LDL and HDL local structures (Fig. 1*B*), we consider that such a situation holds also in the other two temperature regions, $\mathcal{R}_{int}$ and $\mathcal{R}_{LDL}$, where there is the progressive build-up of the expanded tetrahedral HB network with decreasing temperature.

The chemical shift $\delta(T)$ is related to the number of possible configurations of the water molecules in the HB network. Considering that this number is inversely proportional to $\langle N_{HB}\rangle$, according to the entropy definition we can assume $S \approx -k_B \ln\langle N_{HB}\rangle$. Therefore, the temperature derivative of the measured fractional chemical shift,

$$-\left(\frac{\partial \ln\delta(T)}{\partial T}\right)_P \approx -\left(\frac{\partial \ln\langle N_{HB}\rangle}{\partial T}\right)_P \approx \left(\frac{\partial S}{\partial T}\right)_P, \qquad [1]$$

should be proportional to the constant pressure specific heat $C_P(T)$ (being $C_P = T(\partial S/\partial T)_P$), a quantity never experimentally measured in the deep supercooled regime <250 K for liquid bulk water. Fig. 2*A* reports (*Left*) the derivative $-T\partial \ln \delta(T)/\partial T$ obtained from the $\delta(T)$ data of Fig. 1*A*. Also shown are the $C_P(T)$ values measured in bulk water in the interval 244.5 K $< T <$ 290 K (41) and the same quantity obtained by means of a simulation study from the TIP5P model of water for 210 K $< T <$ 290 K (*Right*) (42). All these data display an analogous thermal behavior. In fact, within the error bars, there is good agreement between the C_P data. The "configurational" specific heat obtained from the measured δ and the $C_P(T)$ calculated in simulation display maxima at about the same temperature (≃235 K) of the maximum in $(\partial\rho/\partial T)_P$ (40) upon crossing the Widom line temperature, T_W (Fig. 2*B*) (10, 13, 43). We stress that whereas $(\partial\rho/\partial T)_P$ is directly related to the cross-correlation between the entropy and volume fluctuations $\langle(\Delta S \Delta V)\rangle$, C_P is proportional to the square of the entropy fluctuations. We stress that very recent calorimetric data on water confined in silica gel, which cover the range 100 K $< T <$ 300 K, show a behavior that agrees with our results (44).

To confirm the validity of our approach and the obtained results, we consider δ of the hydration water proton for lysozyme

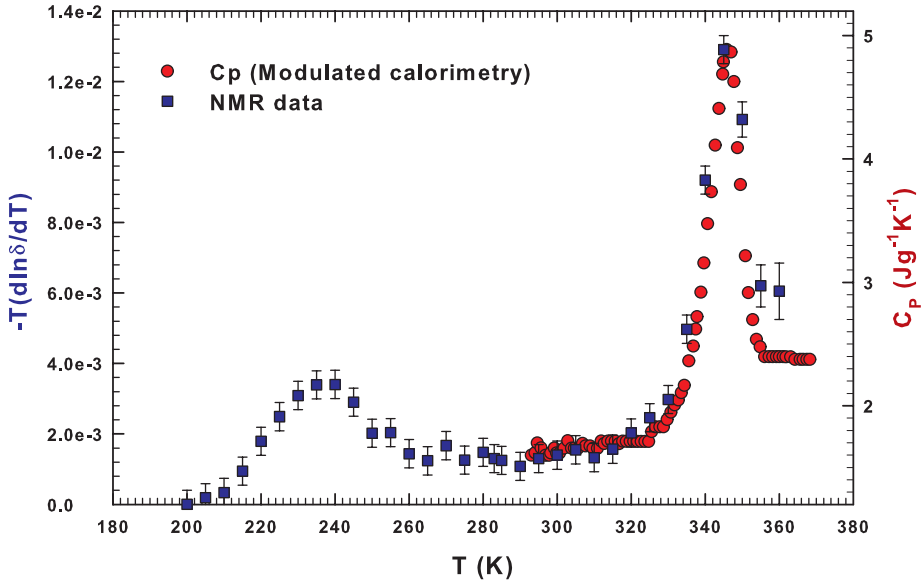

Fig. 3. Test of the argument that the logarithmic temperature derivative of the proton chemical shift is related to the specific heat. The figure, reporting data coming from the water-protein (lysozyme) system, shows a detailed comparison between the present NMR data and previous C_P data (33).

at the hydration level $h = 0.3$, a condition in which only one monolayer of water is supposed to be on the surface of each protein. We have explored the temperature range 200 K < T < 370 K for the following reasons: (*i*) in such a system, water dynamics display the fragile-to-strong cross-over phenomena (FSC) observed in confined and simulated water (32, 42); in particular, the cross-over temperature T_W is nearly coincident among these water confined forms (32, 42); (*ii*) another phenomenon governing biological properties of proteins occurs at high temperatures, just below the onset of protein denaturation. In the first case, the FSC is entirely due to the complete development of the LDL water phase (i.e., of the HB tetrahedral network) located just at the Widom line (32, 42).

A protein is in the native state up to a given temperature and evolves, on increasing T, into a region characterized by a reversible unfolding-folding process. This latter phenomenon depends on the chemical nature of the protein and the solvent. For water-lysozyme it occurs in the range 310 K < T < 360 K. Above 355 K, lysozyme denatures irreversibly. For $h = 0.12$, calorimetric measurements (33) show a broad peak in C_P. The process rate constant varies with T according to an Arrhenius law with an activation energy typical of the HB strength (33), so hydration water appears to play a determinant role also for this transition. In particular, all of the observed data of an experiment characterized by the peak in C_P at $T = 346$ K are consistent with the point of view that the first step of denaturation of a small one-domain globular protein like lysozyme is a reversible conformational (unfolding) transition, and the second step is irreversible. Thus, a dramatic change in the protein structure is driven by the HBs between the protein and its hydration water. This latter quantity is strictly related to δ.

Fig. 3 shows in a double scale plot $(-T\partial \ln \delta(T)/\partial T)_P$ for lysozyme hydration water and the right-hand side of the figure reports C_P measured in the temperature region including the reversible unfolding-folding process. One sees that $(-T\partial \ln \delta(T)/\partial T)$ displays two maxima, the first on crossing the Widom line $T_W(P)$ as proposed by experiments and simulation studies on hydrated proteins (32, 42) and the second at a temperature nearly coincident with the associated protein denaturation process. The first maximum, at ≈240 K, i.e., the same temperature as that of confined water, is a proof that both are due to the same structural change of water. In fact, at T_W the LDL phase dominates water properties (11, 34). Finally, the agreement between δ and C_P, aside from different prefactors, supports the physical idea that both C_P and δ are measures of the temperature derivative of an entropy-like quantity. Because δ is related to orientational local order, as opposed to other translational local order, our finding is consistent with the possibility that the contribution of the orientational disorder to entropy is dominant. Our work is also consistent with molecular dynamics simulations using the TIP5P model, which demonstrate that in protein hydration water and in bulk water, dQ/dT has a maximum at the crossing of the Widom line $T_W(P)$ (35).

In conclusion, the present study introduces NMR proton chemical shift measurements as a new method for estimating the configurational part of the heat capacity $C_P(T)$ that results from the hydrogen bonding of the water molecules. Because the NMR technique also gives the chemical shift of each sample nucleus with non-zero spin, such an approach may be applicable to more complex materials.

Methods

It is widely known that the chemical shift δ is an assumed linear response of the electronic structure of a system under investigation to an external magnetic field B_0, as $B(j) = (1 - \delta_j)B_0$, where j is an index identifying the chemical environment (45, 46). It is measured in an NMR experiment by the free induction decay (FID),[‖] and specifically, it is related to the magnetic shielding tensor σ, which in turn relates to the local field experienced by the magnetic moment of the observed nucleus. The magnetic shielding tensor σ, strongly dependent on the local electronic environment, is a useful probe of the local geometry and, in particular, for the hydrogen bond structure for water and aqueous systems and solutions (47). Of interest to us are the isotropic parts, $\sigma_{iso} \equiv \mathrm{Tr}(\sigma/3)$, and the shielding anisotropy $\Delta\sigma \equiv \sigma_{33} - (\sigma_{11} + \sigma_{22})/2$, where σ_{11}, σ_{22}, and σ_{33} are the three principal components of σ. σ_{iso} is experimentally obtained via the measured proton chemical shift relative to a reference state through the relation (48).

[‖]In the early days, NMR technique was only used to accurately measure the nuclear magnetic moment. After the discovery of the chemical shift effect the technique was used by the chemical physics community. In fact the FID contains information about the set of all nuclear species in the studied sample whose resonance frequencies lie within the harmonic content of the NMR radio frequency (RF) pulse. Thus, NMR, by means of the chemical shift δ, is selective of the nucleus chosen to be studied and is highly sensitive to its local environment

$$\delta = \sigma_{\rm iso}^{\rm ref} - \sigma_{\rm iso} + \left(A - \frac{1}{3}\right)(\chi^{\rm ref} - \chi). \qquad [2]$$

Here, χ is the magnetic susceptibility, and the factor A depends on the sample shape and orientation: $A = 1/3$ for a spherical sample. Because the magnetic field exerted on a proton is $B_0[1 + (4\pi/3)\chi(T)]$, the resonance frequency is $\omega(T) = \gamma H_0[1 - \sigma(T) + (4\pi/3)\chi(T)]$, where γ is the proton gyromagnetic ratio. Thus, the deviation of $\sigma(T)$ from a reference value gives $\delta(T)$. Because the magnetic susceptibility per water molecule, χ_0, can be assumed to be T and P independent, $\chi(T)$ is simply given by $\chi_0\rho(T)$, where $\rho(T)$ is the density at a temperature T. In the liquid and gas phases, $\omega(T)$ and $\rho(T)$ can be obtained directly from the experiment. Considering that water molecules in the gas phase at 473 K are isolated, we can set $\delta_g(473\ {\rm K}) = 0$, where g indicates the gas. Thus, $\delta(T) = (\omega(T) - \omega_g)/\omega_g - (4\pi/3)\chi_0(\rho(T) - \rho_g)$. Thus, $\delta(T)$ can be determined from $\omega(T)$ and $\rho(T)$. Hence, an isolated water molecule in a dilute gas can be taken to be the reference for δ, so that δ represents the effect of the interaction of water with the surroundings providing, in particular, a rigorous picture of the intermolecular geometry (14). In liquid water, the shielding tensor is isotropically averaged by fast molecular tumbling, so the NMR frequency provides information only on $\sigma_{\rm iso}$. In addition, the $\Delta\sigma$ contribution escapes detection because ^{1}H relaxation is heavily dominated by the strong magnetic dipole field from nearby protons (49). However, δ is directly related to the average number of local configurations in which a water molecule is involved (14–17). The water proton chemical shift has been studied in the same confined geometry used in the previous experiments. The confining substrate is a micelle-templated mesoporous silica matrix MCM-41-S comprised of quasi-1D cylindrical tubes arranged in a hexagonal structure, synthesized by using the zeolite seeds method (8–11). We study two different samples having tube diameters of $d = 2.4$ nm and 1.4 nm. Both have hydration levels of $h \simeq 0.5$ g of H_2O per gram of MCM-41-S. We perform static NMR experiments at ambient pressure P in the temperature interval $195\ {\rm K} < T < 293\ {\rm K}$ by using a Bruker AVANCE NMR spectrometer operating at 700 MHz proton resonance frequency. At $h \simeq 0.5$ both samples are fully hydrated and the measured $\delta(T)$ are, within the experimental uncertainty of ± 0.05 ppm, pore size independent. As can be observed in Fig. 1*A*, at lower T there is a round-off in $\delta(T)$ with a possible maximum at $\approx$215 K. However, such a situation (which is not relevant to the present study) deserves special care, so we planned a magic angle spinning (MAS-NMR) experiment. The second studied system consists of the first-shell hydration water of lysozyme. In that case we have used hen egg white lysozyme obtained from Fluka (L7651 three times crystallized, dialysed, and lyophilized) and used without further purification. Samples were dried, hydrated isopiestically and controlled by means of a precise procedure (32). We used protein-water samples with hydration levels $h = 0.3$. The configurational heat capacity, obtained from $\delta(T)$ by means of Eq. **1**, is plotted on the left-hand sides of Figs. 2*A* and 3. The comparison with respect to the measured C_P values is made by means of a double scale plot (on the right-hand side of these figures). The only difference is one adjustable parameter: the amplitude of the signal.

ACKNOWLEDGMENTS. We thank G. Johari for important critical comments. The research at MIT is supported by the Materials Science Division of the U.S. Department of Energy. The research at Messina is supported by the MURST-PRIN2004. We benefited from affiliation with the EU Marie Curie Research and Training Network on Arrested Matter (contract no. MRT-CT2003-504712); in particular, N.G.S. and J.S. are supported by research fellowships thereof. H.E.S. is supported by NSF Chemistry grant CHE0616489.

1. Angell CA (1982) in *Water*: A *Comprehensive Treatise*, ed Franks F (Plenum, New York), Vol 7, pp 1–81.
2. Mishima O, Stanley HE (1998) The relationship between liquid, supercooled and glassy water. *Nature* 396:329–334.
3. Debenedetti PG, Stanley HE (2003) Supercooled and glassy water. *Physics Today* 56:40–46.
4. Poole PH, Sciortino F, Essmann U, Stanley HE (1992) Phase behaviour of metastable water. *Nature* 360:324–328.
5. Moynihan CT (1997) Two species/nonideal solution model for amorphous/amorphous phase transitions. *Mater Res Soc Symp Proc* 455:411–425.
6. Poole PH, Sciortino F, Grande T, Stanley HE, Angell CA (1994) Effect of hydrogen bonds on the thermodynamic behavior of liquid water. *Phys Rev Lett* 73:1632–1635.
7. Borick SS, Debenedetti PG, Sastry S (1995) A lattice model of network-forming fluids with orientation-dependent bonding: equilibrium, stability, and implications for the phase behavior of supercooled water. *J Phys Chem* 99:3781–3793.
8. Liu L, Chen S-H, Faraone A, Yen CW, Mou CY (2005) Pressure dependence of fragile-to-strong transition and a possible second critical point in supercooled confined water. *Phys Rev Lett* 95:117802.
9. Mallamace F, *et al.* (2006) The fragile-to-strong dynamic crossover transition in confined water: nuclear magnetic resonance results. *J Chem Phys* 124:161102.
10. Chen S-H, *et al.* (2006) The violation of the Stokes-Einstein relation in supercooled water. *Proc Natl Acad Sci USA* 103:12974–12978.
11. Mallamace F, *et al.* (2007) Evidence of the existence of the low-density liquid phase in supercooled, confined water. *Proc Natl Acad Sci USA* 104:424–428.
12. Xu LM, *et al.* (2005) Relation between the Widom line and the dynamic crossover in systems with a liquid-liquid phase transition. *Proc Natl Acad Sci USA* 102:16558–16562.
13. Kumar P, *et al.* (2007) Relation between the Widom line and the breakdown of the Stokes-Einstein relation in supercooled water. *Proc Natl Acad Sci USA* 104:9575–9579.
14. Matubayasi M, Wakai C, Nakahara M (1997) NMR study of water structure in super- and subcritical conditions. *Phys Rev Lett* 78:2573–2576.
15. Modig K, Halle B (2002) Proton magnetic shielding tensor in liquid water. *J Am Chem Soc* 124:12031–12041.
16. Modig K, Pfrommer BG, Halle B (2003) Temperature-dependent hydrogen-bond geometry in liquid water. *Phys Rev Lett* 90:075502.
17. Sebastiani D, Parrinello M (2002) Ab-initio study of NMR chemical shifts of water under normal and supercritical conditions. *Chem Phys Chem* 3:675–679.
18. Svishchev IM, Kusalik PG (1993) Proton chemical shift of water in the liquid state: computer simulation results. *J Am Chem Soc* 115:8270–8274.
19. Gun'ko VM, Turov VV (1999) Structure of hydrogen bonds and ^{1}H NMR spectra of water at the interface of oxides. *Langmuir* 15:6405–6415.
20. Muller N (1965) Concerning structural models for water and chemical-shift data. *J Chem Phys* 43:2555–2556.
21. Hindman JC (1966) Proton resonance shift of water in the gas and liquid states. *J Chem Phys* 44:4582–4592.
22. Hoffmann MM, Conradi MS (1997) Are there hydrogen bonds in supercritical water? *J Am Chem Soc* 119:3811–3817.
23. Stanley HE, Teixeira J (1980) Interpretation of the unusual behavior of H_2O and D_2O at low temperatures: tests of a percolation model. *J Chem Phys* 73:3404–3422.
24. Oleinikova A, Brovchenko I (2006) Percolating networks and liquid-liquid transitions in supercooled water. *J Phys Cond Matt* 18:S2247–S2259.
25. Speedy RJ (1982) Stability-limit conjecture. An interpretation of the properties of water. *J Phys Chem* 86:982–991.
26. Burton EF, Oliver WF (1936) The crystal structure of ice at low temperatures. *Proc R Soc Lond A* 153:166–172.
27. Mishima O, Calvert LD, Whalley E (1984) Melting ice I at 77 K and 10 kbar: a new method of making amorphous solids. *Nature* 310:393–395.
28. Mishima O, Calvert LD, Whalley E (1985) An apparently first-order transition between two amorphous phases of ice induced by pressure. *Nature* 314:76–78.
29. Soper AK, Ricci MA (2000) Structures of high-density and low-density water. *Phys Rev Lett* 84:2881–2884.
30. Buldyrev SV, Kumar P, Debenedetti PG, Rossky PJ, Stanley HE (2007) Water-like solvation thermodynamics in a spherically symmetric solvent model with two characteristic lengths. *Proc Natl Acad Sci USA* 104:20177–20182.
31. Yan ZY, *et al.* (2007) Structure of the first-and second-neighbor shells of simulated water: quantitative relation to translational and orientational order. *Phys Rev E* 76:051201.
32. Chen S-H, *et al.* (2006) Observation of fragile-to-strong dynamic crossover in protein hydration water. *Proc Natl Acad Sci USA* 103:9012–9016.
33. Salvetti G, Tombari E, Mikheeva L, Johari GP (2002) The endothermic effects during denaturation of lysozyme by temperature modulated calorimetry and an intermediate reaction equilibrium. *J Phys Chem B* 106:6081–6087.
34. Mallamace F, *et al.* (2007) Role of the solvent in the dynamical transitions of proteins: the case of the lysozyme-water system. *J Chem Phys* 127:045104.
35. Kumar P, *et al.* (2006) Glass Transition in biomolecules and the liquid-liquid critical point of water. *Phys Rev Lett* 97:177802.
36. Oleinikova A, Smolin N, Brovchenko I (2007) Influence of water clustering on the dynamics of hydration water at the surface of a lysozyme. *Biophys J* 93:2986–3000.
37. Lagi M, *et al.* (2008) The low-temperature dynamic crossover phenomenon in protein hydration water: simulations vs experiments. *J Phys Chem B* 112:1571–1575.
38. Angell CA, Shuppert J, Tucker JC (1973) Anomalous properties of supercooled water. Heat capacity, expansivity, and proton magnetic resonance chemical shift from 0 to −38%. *J Phys Chem* 77:3092–3099.
39. Pfrommer BG, Mauri F, Louie SG (2000) NMR chemical shifts of ice and liquid water: the effects of condensation. *J Am Chem Soc* 122:123–129.
40. Mallamace F, *et al.* (2007) The anomalous behavior of the density of water in the range $30\ {\rm K} \leq T \leq 373$ K. *Proc Natl Acad Sci USA* 104:18387–18391.
41. Tombari E, Ferrari C, Salvetti G (1999) Heat capacity anomaly in a large sample of supercooled water. *Chem Phys Lett* 300:749–751.
42. Stanley HE, *et al.* (2007) The puzzling unsolved mysteries of liquid water: some recent progress. *Phys A* 386:729–743.
43. Franzese G, Stanley HE (2007) The Widom line of supercooled water. *J Phys Cond Matt* 19:205126.
44. Oguni M, Maruyama S, Wakabayashi K, Nagoe A (2007) Glass transitions of ordinary and heavy water within silica-gel nanopores. *Chem Asian J* 2:514–520.
45. Purcell EM, Torrey HC, Pound RV (1946) Resonance absorption by nuclear magnetic moments in a solid. *Phys Rev* 69:37–38.
46. Bloch F (1946) Nuclear induction. *Phys Rev* 70:460–474.
47. Becker ED (1996) *Encyclopedia of Nuclear Magnetic Resonance*, eds Grant DM, Harris RK (Wiley, Chichester), p 2409.
48. Grant DM (1996) *Encyclopedia of Nuclear Magnetic Resonance*, eds Grant DM, Harris RK (Wiley, Chichester), p 1298.
49. Abragam A (1961) *The Principles of Nuclear Magnetism* (Clarendon, Oxford).